5

Chapter 5

5.1 Flexoelectric Studies on Mixtures of Rod-like and Bent-core Molecules

Splay or bend distortion of a nematic liquid crystal can create an electric *polarization*. This was first shown by Meyer[16] and this effect is known as flexoelectric effect. The flexoelectric polarization **P** induced by a weak distortion of a nematic director field is given by,

$$\mathbf{P} = e_1 \left(\boldsymbol{\nabla} . \mathbf{n}\right) \mathbf{n} + e_3 \left(\boldsymbol{\nabla} \times \mathbf{n}\right) \times \mathbf{n} \tag{5.1}$$

where e_1 and e_3 are flexoelectric coefficients corresponding to the splay and bend distortions respectively with the dimensions of charge/length or electric potential and of *arbitrary sign*. This expression is the most general polar vector that can be constructed from the *apolar* director

n. On the basis of Meyer's model[16] only nematics made up of *polar* molecules with *shape anisotropy* can be expected to exhibit flexoelectric polarization under deformation. In the undistorted state[Figure 5.1(a),5.2(a)] because of the equal probability of both orientations, the dipole moments of the individual molecules cancel one another and the net dipole moment is zero. Let a nematic be made of pear or wedge shaped molecules with longitudinal dipole moments [see Figure 5.1(a)]. If the system is deformed with *splayed* director [Figure 5.1(b)], the efficient packing of the molecules generates a net dipole moment, resulting in a macroscopic polarization. A similar type of effect is also observed in a nematic made of banana shaped molecules with transverse dipole moments [see Figure 5.2(a)] subjected to a bend distortion [Figure 5.2(b)].

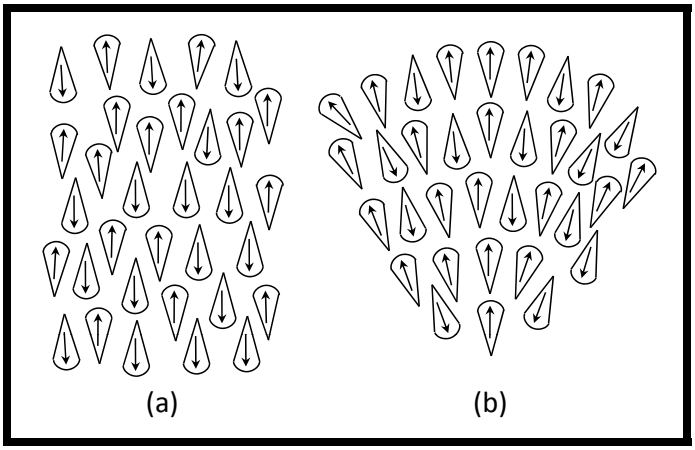

FIGURE 5.1: A nematic consisting of pear-shaped molecules with longitudinal dipole moments becomes polarized under splay deformation

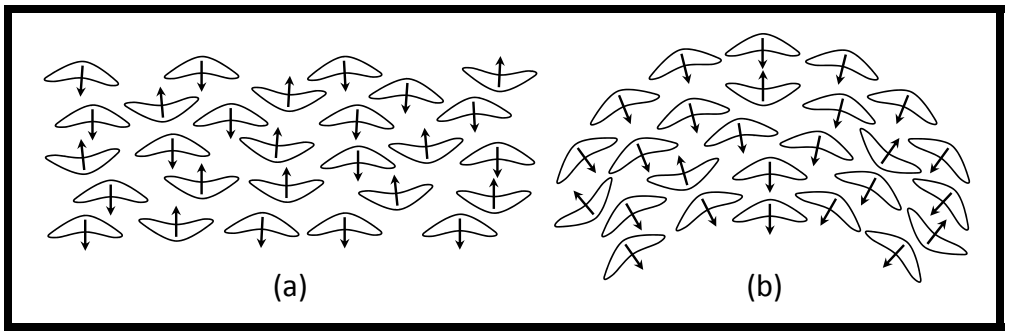

FIGURE 5.2: A nematic consisting of banana-shaped molecules with transverse dipole moments becomes polarized under bend deformation

Later Prost and Marcerou[17] showed that the quadrupole density of the medium also contributes to the flexoelectric effect. This contribution is independent of the molecular shape. The nematogenic molecules generally have non-zero quadrupole moments, hence *flexoelectricity is a universal property of all nematics*. The quadrupolar contribution is comparable in magnitude to the dipolar contribution. To understand the origin of the quadrupolar contribution, we consider a stack of quadrupoles (see Figure 5.3a). Due to the symmetry of the packing, there is no net dipole moment in region 2. In Figure 5.3(b), if the structure is splayed, we can see that there is a net dipole moment in region 2 and the medium becomes polarized.

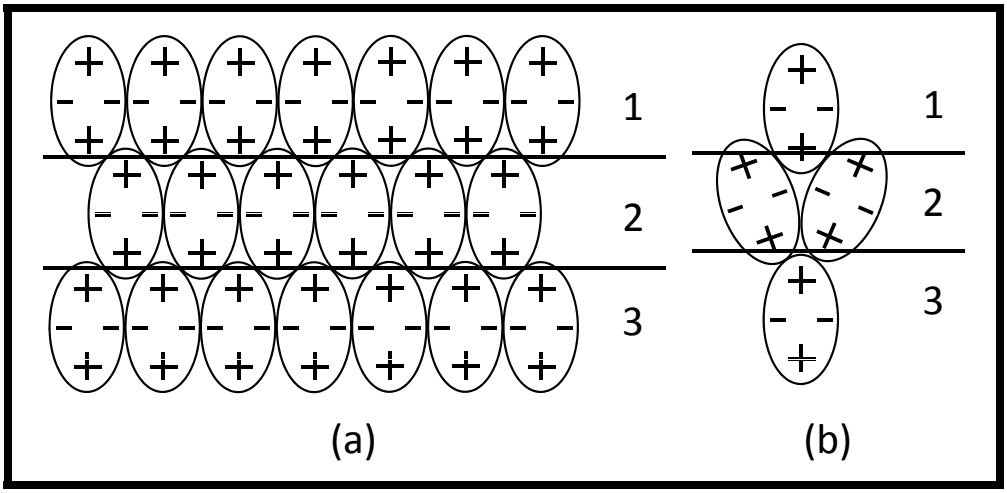

Figure 5.3: (a) A stack of quadrupoles. Because of the symmetry of the arrangement of the quadrupoles there is no bulk polarization. (b) The structure becomes polarized if subjected to a splay distortion.

A large number of theoretical papers on the relationship between the flexoelectric effect and the orientational order parameter (S) have been published[61–65]. If the molecular structure is rigid the phenomenological model shows that the dipolar contribution to e_1 and e_3 varies as S^2[61–63]. And the main term from the quadrupole density varies as S[17]. Osipov's[62] detailed molecular calculation shows that the flexoelectric coefficients have terms depending on both S and S^2. The difference in the flexoelectric coefficients ($e_1 - e_3$) is mainly determined by the dipolar contribution.

There have been several measurements of flexoelectric coefficients of nematics[66–75], using many techniques. Marcerou *et al.* devised a technique to measure the intensity of light scattering

generated by the spatially periodic flexoelectric distortion due to an applied AC field[17]. They measured $|e_1 + e_3|$ of a symmetric tolane which does not have a dipolar contribution and value of $|e_1+e_3|$ arising from the quadrupole moments. Dozov *et al.* [67, 76] devised a simple experimental technique of measuring $e^* = (e_1 - e_3)$ which arises mainly from the dipolar contribution to flexoelectricity. 8CB (4-octyl-4′-cyanobiphenyl) has strong longitudinal dipole moment for C≡N group and MBBA (4-methoxybenzylidene-4′-butylaniline) has large lateral dipole. For both 8CB and MBBA $e^* \propto S^2$ which arises due to the dipolar contribution[67]. 8OCB (4-*n*-octyloxy 4′-cyanobiphenyl) has strong longitudinal dipole moment for terminal C≡N group and 8 carbon chain giving rise to a transverse component of the dipole moment. The sign of e^*/K is negative, where K is elastic constant. The magnitude of e^*/K increases with increase of temperature and e^* is proportional to S though it is dependent on the dipolar effect and the result was attributed to the flexibility of the 8 carbon atom chain[67] ($K \propto S^2$ in the mean field theory).

Recently Harden *et al.* [75] have measured the flexoelectric coefficients of pure bent-core nematic 4-chloro-1,3-phenylene bis 4-[4′-(9-decenyloxy) benzoyloxyl] benzoate (C1Pbis10BB) by a different technique where an oscillatory bend deformation is induced by periodically flexing a thin layer of NLCs contained between nonrigid conducting surfaces and then measure the induced electric voltage which is generated by the e_3 coefficient. The magnitude of e_3 was found to be *3 orders of magnitude larger than in calamitics*.

We are interested in measuring flexoelectric coefficients of nematic mixtures made of 8OCB (R) and BC12 (BC) (see Figure 4.4) molecules. The mixtures exhibit large nematic ranges (see Figure 3.5). Using the Dozov technique[76] we have measured e^*/K of pure 8OCB, 5M and 8M mixtures. The signs of e^*/K of 8OCB and the two mixtures are all negative. In magnitude, e^*/K of 5M is ∼2 times larger than that of pure 8OCB. From this data we get, $\left(\frac{e^*}{K}\right)_{\text{BC}} \approx 20 \left(\frac{e^*}{K}\right)_{\text{8OCB}}$, which is very much smaller than Harden's[75] result.

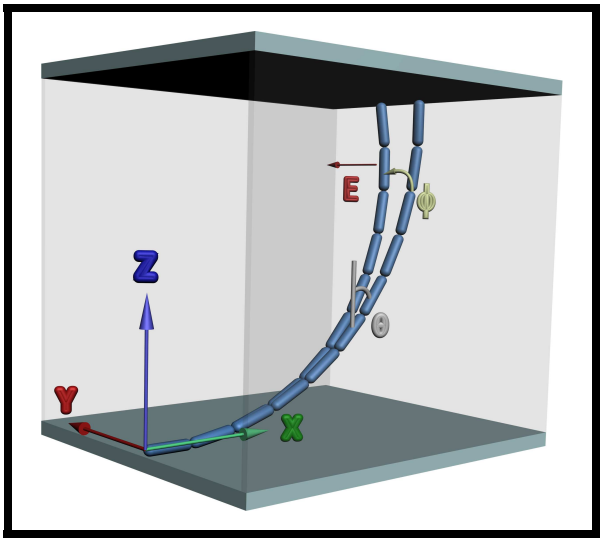

Figure 5.4: The geometry of the HAN cell used to measure e^*/K. A dc electric field **E** is applied along the Y axis produces a twist distortion.

5.2 Measurement of $(e_1 - e_3)$ Using a Hybrid Aligned Nematic Cell

Consider a hybrid aligned cell[76], with bottom plate coated for homogeneous alignment and the top plate coated to get homeotropic alignment(Figure 5.4). The anchoring at the two surfaces is assumed to be strong. The director field in such a cell has a permanent *splay-bend distortion*, which generates flexoelectric polarization **P**. Two wire electrodes are also used as spacers to apply a field perpendicular to the plane of the distorted director. At the bottom plate, $(z = 0)$ the director is along the X axis and the tilt angle reduces continuously on moving towards the upper plate $(z = L)$ where the director is oriented along the Z axis. Here L is the cell thickness. The tilt angle θ is a function of the coordinate z. If a uniform dc electric field **E** is applied along the Y axis, a twist distortion is produced in the medium due to the action of **E** on **P** and the flexoelectric effect contributes to the bulk torque density. Under the action of **E**, the director continuously twists, getting a component along the Y axis with the twist angle ϕ also being a function of z.

The equation for the director can be written as,

$$\mathbf{n}(z) = \sin\theta(z)\cos\phi(z)\,\hat{i} + \sin\theta(z)\sin\phi(z)\,\hat{j} + \cos\theta(z)\,\hat{k} \tag{5.2}$$

The electric field is given by,

$$\mathbf{E} = E\,\hat{j} \tag{5.3}$$

As θ and ϕ are both functions of z only, we can write,

$$\boldsymbol{\nabla} = \hat{k}\frac{d}{dz} \tag{5.4}$$

From Equation (5.1) we get the flexoelectric polarization,

$$\begin{aligned}\mathbf{P} &= \left[\left(e_3\cos^2\theta - e_1\sin^2\theta\right)\cos\phi\,\frac{d\theta}{dz} - e_3\cos\theta\sin\theta\sin\phi\,\frac{d\phi}{dz}\right]\hat{i} \\ &\quad + \left[\left(e_3\cos^2\theta - e_1\sin^2\theta\right)\sin\phi\,\frac{d\theta}{dz} + e_3\cos\theta\sin\theta\cos\phi\frac{d\phi}{dz}\right]\hat{j} \\ &\quad - \left[\left(e_1+e_3\right)\cos\theta\sin\theta\,\frac{d\theta}{dz}\right]\hat{k}\end{aligned} \tag{5.5}$$

If there is no external field, the twist angle $\phi = 0$. The polarization vector also depends on z. For $\theta \to 0$ (*ie.*, upper plate) and $\theta \to \pi/2$ (*ie.*, lower plate) respectively we get,

$$\mathbf{P}_{\theta\to 0} = e_3\,\frac{d\theta}{dz}\,\hat{i} \quad \text{and} \quad \mathbf{P}_{\theta\to\pi/2} = -e_1\,\frac{d\theta}{dz}\,\hat{i} \tag{5.6}$$

$d\theta/dz < 0$, and the directions of polarization $\mathbf{P}$, are as shown in Figure 5.5 for positive e_1 and e_3.

The flexoelectric energy density is given by,

$$\begin{aligned}W_P &= -\mathbf{P}\,.\,\mathbf{E} \\ &= -\left[\left(e_3\cos^2\theta - e_1\sin^2\theta\right)\sin\phi\,\frac{d\theta}{dz} + e_3\cos\theta\cos\phi\sin\theta\,\frac{d\phi}{dz}\right]E\end{aligned} \tag{5.7}$$

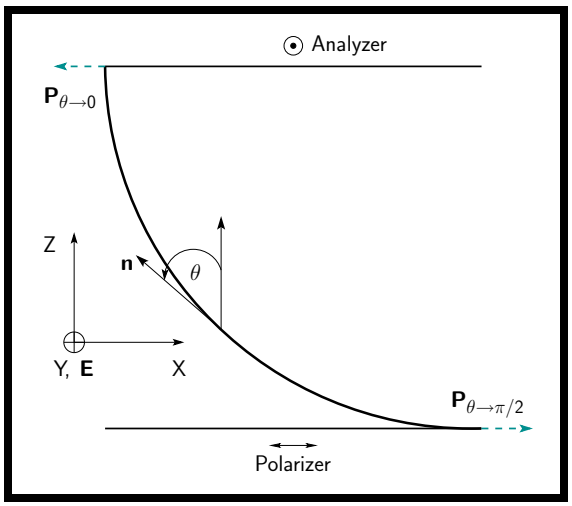

Figure 5.5: Director profile in the cell in the absence of **E**. The polarization vectors at the two walls for e_1 and $e_3 > 0$ are also shown.

The elastic energy density is given by,

$$\begin{aligned} \mathsf{W}_{\mathsf{el}} &= \frac{1}{2}K_{11}\big[\boldsymbol{\nabla}.\,\mathbf{n}\big]^2 + \frac{1}{2}K_{22}\big[\mathbf{n}\,.\boldsymbol{\nabla}\times\mathbf{n}\big]^2 + \frac{1}{2}K_{33}\big[\mathbf{n}\times\boldsymbol{\nabla}\times\mathbf{n}\big]^2 \\ &= \frac{1}{16}\Bigg[4\big\{K_{11}+K_{33}+(K_{33}-K_{11})\cos 2\theta\big\}\left(\frac{d\theta}{dz}\right)^2 + \\ &\quad \big\{3K_{22}+K_{33}-4K_{22}\cos 2\theta-(K_{33}-K_{22})\cos 4\theta\big\}\left(\frac{d\phi}{dz}\right)^2\Bigg] \end{aligned} \tag{5.8}$$

The dielectric energy density, $-\frac{\Delta\epsilon}{8\pi}(\mathbf{E}.\mathbf{n})^2 \propto E^2$ and can be neglected for small values of **E**, in comparison with the flexoelectric energy density $\propto E$.

The total energy density, $\mathcal{L} = \mathsf{W}_{\mathsf{P}} + \mathsf{W}_{\mathsf{el}}$ and the total energy per unit area,

$$\mathsf{W} = \int_0^L \mathcal{L}\,dz \tag{5.9}$$

As there are two variables θ and ϕ, we need two Euler-Lagrange equations to minimize the energy,

$$\frac{\partial\mathcal{L}}{\partial\theta} - \frac{d}{dz}\left(\frac{\partial\mathcal{L}}{\partial\theta'}\right) = 0 \tag{5.10}$$

$$\frac{\partial \mathcal{L}}{\partial \phi} - \frac{d}{dz}\left(\frac{\partial \mathcal{L}}{\partial \phi'}\right) = 0 \tag{5.11}$$

where $\theta' = d\theta/dz$ and $\phi' = d\phi/dz$. Inserting $\mathcal{L}$ in Equation (5.10) and Equation (5.11) we get respectively,

$$2(K_{33} - K_{11})\sin 2\theta \left(\frac{d\theta}{dz}\right)^2 - 4(e_1 - e_3)E\cos\phi\sin^2\theta \left(\frac{d\phi}{dz}\right) + \Big\{2K_{22}\sin 2\theta + (K_{33} - K_{22})\sin 4\theta\Big\}\left(\frac{d\phi}{dz}\right)^2 - 2\Big\{K_{11} + K_{33} + (K_{33} - K_{11})\cos 2\theta\Big\}\left(\frac{d^2\theta}{dz^2}\right) = 0 \tag{5.12}$$

and

$$\left[4(e_3 - e_1)E\cos\phi\sin\theta + 8\cos\theta\Big\{K_{22} + (K_{33} - K_{22})\cos 2\theta\Big\}\left(\frac{d\phi}{dz}\right)\right]\left(\frac{d\theta}{dz}\right) + \Big\{(3K_{22} + K_{33})\sin\theta + (K_{33} - K_{22})\sin 3\theta\Big\}\left(\frac{d^2\phi}{dz^2}\right) = 0 \tag{5.13}$$

In our experiment we have used 8OCB, 5M and 8M mixtures. K_{33}/K_{11} of 8OCB and 5M are 1.6 and 0.8 at about $\mathsf{T} - \mathsf{T}_{\mathsf{NI}} = -10^{\circ}\mathsf{C}$ respectively (see Figures 3.11 and 3.12 of Chapter 3). For simplicity we consider the one constant approximation ($K_{11} = K_{22} = K_{33} = K$). Equations (5.12) and (5.13) respectively become,

$$K\left[\left(\frac{d^2\theta}{dz^2}\right) - \sin\theta\cos\theta\left(\frac{d\phi}{dz}\right)^2\right] = -(e_1 - e_3)E\sin^2\theta\cos\phi\left(\frac{d\phi}{dz}\right) \tag{5.14}$$

and

$$K\sin^2\theta\left(\frac{d^2\phi}{dz^2}\right) + 2K\sin\theta\cos\theta\left(\frac{d\theta}{dz}\right)\left(\frac{d\phi}{dz}\right) = (e_1 - e_3)E\cos\phi\sin^2\theta\left(\frac{d\theta}{dz}\right)$$

or,

$$\frac{d}{dz}\left(K\sin^2\theta\frac{d\phi}{dz}\right) = (e_1 - e_3)E\cos\phi\sin^2\theta\left(\frac{d\theta}{dz}\right) \tag{5.15}$$

In the absence of electric field, the twist angle $\phi = 0$, and the Equation (5.14) reduces to,

$$\left(\frac{d\theta}{dz}\right) = C_1 z + C_2 \tag{5.16}$$

where C_1 and C_2 are two integration constants which can be evaluated by the boundary conditions. In the bend-splay distortion the boundary conditions are, $\theta(z = 0) = \pi/2$ and $\theta(z = L) = 0$. We get the functional form of θ ,

$$\boxed{\theta(z) = \frac{\pi}{2}\left(1 - \frac{z}{L}\right)} \tag{5.17}$$

The azimuthal Equation (5.15) gives the twist angle $\phi(z)$. For low fields, ϕ is a linear function of E. To calculate the twist angle ϕ, Equation (5.15) is linearized.

$$\begin{aligned}
\frac{d}{dz}\left(K\sin^2\theta\,\frac{d\phi}{dz}\right) &= (e_1 - e_3)E\sin^2\theta\left(\frac{d\theta}{dz}\right) \\
\text{or, } \frac{d}{d\theta}\left(K\sin^2\theta\,\frac{d\phi}{dz}\right) &= (e_1 - e_3)E\sin^2\theta \\
\text{or, } K\sin^2\theta\left(\frac{d\phi}{dz}\right) &= \frac{(e_1 - e_3)E}{2}\left(\theta - \frac{\sin 2\theta}{2}\right) \\
\text{or, } K\sin^2\theta\left(\frac{d\phi}{d\theta}\,\frac{d\theta}{dz}\right) &= \frac{(e_1 - e_3)E}{2}\left(\theta - \frac{\sin 2\theta}{2}\right)
\end{aligned}$$

Inserting the value of $(d\theta/dz)$ from Equation (5.17) we get,

$$\left(\frac{d\phi}{d\theta}\right) = \left[\frac{(e_1 - e_3)E\,L}{\pi\,K}\right]\left(\frac{\sin 2\theta}{2} - \theta\right)\Big/\sin^2\theta \tag{5.18}$$

Integrating we get the twist angle $\phi(z)$,

$$\begin{aligned}
\int_0^{\phi(z)} d\phi &= \left[\frac{(e_1 - e_3)E\,L}{\pi\,K}\right]\int_{\pi/2}^{\theta(z)}\left(\frac{\sin 2\theta}{2} - \theta\right)\frac{1}{\sin^2\theta}\,d\theta \\
\text{or, } \phi(z) &= \left[\frac{(e_1 - e_3)E\,L}{\pi\,K}\right]\theta(z)\cot\theta(z)
\end{aligned} \tag{5.19}$$

The largest value $\phi(L)$ close to the upper plate $(z = L)$ is given by,

$$\phi(L) = \frac{(e_1 - e_3) E\, L}{\pi\, K} \tag{5.20}$$

or,

$$\boxed{\frac{(e_1 - e_3)}{K} = \frac{e^*}{K} = \frac{\pi}{E\, L}\, \phi(L)} \tag{5.21}$$

where $e^* = e_1 - e_3$. If Δn and the sample thickness L are sufficiently large, as argued by Dozov *et al.* [76], the plane of polarization of the incident light beam is rotated by $\simeq \phi(L)$, which is directly proportional to E. Thus $(e_1 - e_3)/K$ can be measured by measuring $\phi(L)$ as a function of an applied DC electric field E.

5.3 Experimental Technique

We have used the method of Dozov *et al.* [76] for the measurement of e^*/K. The cell geometry is shown in Figure 5.4. The hybrid aligned cell is constructed by using a SiO coated bottom plate with homogeneous alignment and a top plate coated with ODSE (octadecyl triethoxy silane) to get homeotropic alignment. Two electrodes which are flat stainless steel wires are placed $\sim$ 1mm apart on the bottom plate, such that the wires are parallel to the director on this plate (see Figure 5.4). The thickness of each wire is $\sim$ 25μm. The liquid crystal sample is filled in the isotropic phase by capillary flow and it is kept inside a heater (Mettler FP2). The whole system is placed on the stage of a polarizing microscope. The polarizer and analyzer are in crossed position and the director plane is set parallel to the polarizer. In any HAN cell, there are some domains in which the director distortion can be described as $+\pi/2$ to 0 and others in which it is $-\pi/2$ to 0. These are separated by walls. We choose a region with a single type of domain. The actual distortion is determined by sending a light beam at an angle to the vertical (see Figure 5.6). In one domain, the path length decreases, while it increases in other domain. Thus by using a tilting compensator, the actual sense of distortion can be determined.

To measure the twist angle ϕ a DC electric field is applied between the wires. The liquid crystal samples usually have ionic impurities. When a DC electric field is applied, $+$vely charged ions get attracted to the $-$ve electrode and vice versa. This in turn reduces the electric field in

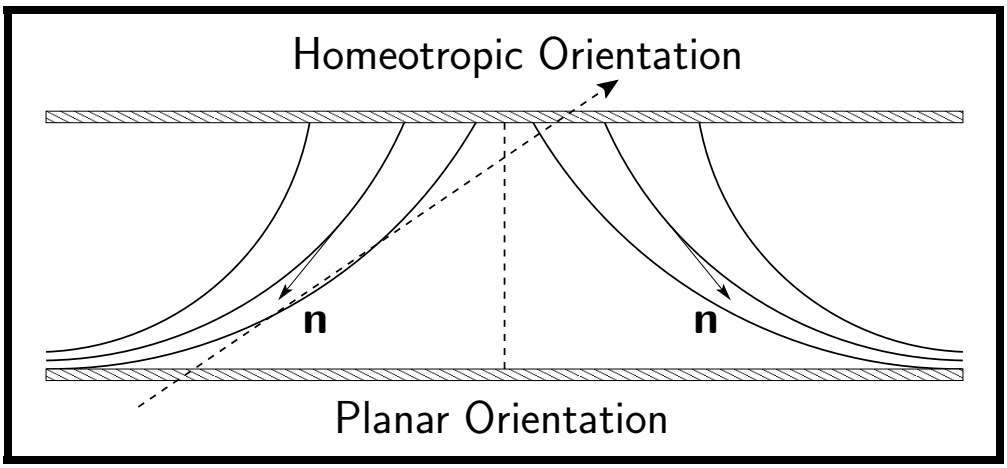

FIGURE 5.6: Two types of distortions in HAN cell. An obliquely incident light beam is used to determine the sign of distortion.

the center. To overcome this problem we have used a double pole double throw (DPDT) switch and frequently changed the sign of the applied DC field before each measurement, which is made quickly after the last change of sign. With applied DC field, the plane of polarization rotates and the rotation of angle is measured by using the analyzer. The angle gives the twist angle at the upper plate *ie.*, $\phi(L)$.

5.4 Results

The twist angle as a function of the applied DC field is shown in Figure 5.7. The signs of $(e_1 - e_3)/K$ of pure 8OCB and the two mixtures are the same, *viz.* negative. As $K \propto S^2$, e^*/K can be expected to be independent of temperature. The decrease in the magnitude of e^*/K as the temperature is lowered in all cases arises becauses K actually increases more than that predicted by the mean field model. As the N-SmA_d transition point is approached, K_{33} diverges, leading to the small values of e^*/K. In magnitude, e^*/K of 5M mixture is ~ 2 times larger than that of pure 8OCB (see Figure 5.8). In 8M mixture at high temperatures, e^*/K is relatively constant and decreases rapidly only close to the T_{NA}. The mixtures with even higher concentrations of BC molecules were aligned only homeotropically and we could not make any measurements. In the 8M mixture the value of e^*/K calculated using Equation (5.21) is lower

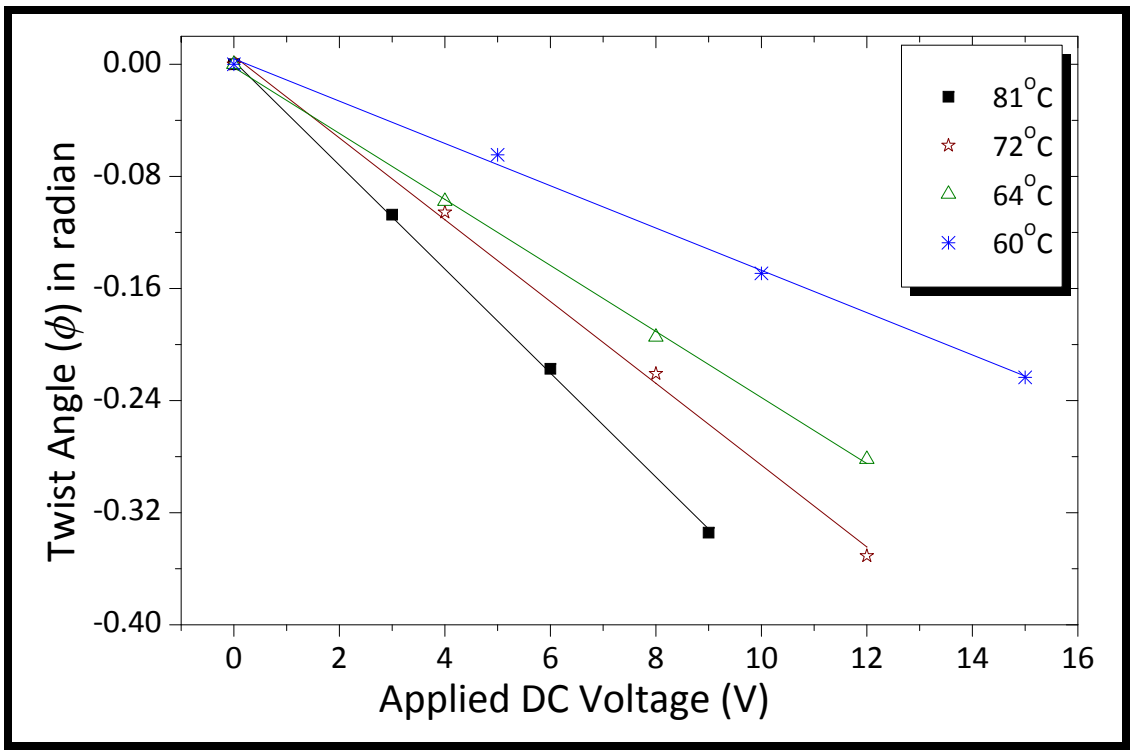

FIGURE 5.7: The electric field variations of the twist angle $\phi(L)$ of 5M mixture at various temperatures. The slope of the straight line decreases with decrease of temperature.

than that of 5M mixture. This is merely a consequence of the fact that even in 8M, at the bottom plate treated for homogeneous alignment, the director has a *large pretilt angle*. The director **n** bends much less than $\pi/2$ to 0 in the cell. This effectively reduces the twist angle ϕ and hence the calculated values of e^*/K decreases and e^*/K of 8M mixture is underestimated.

Indeed, if the tilt angle at the lower plate is θ_0 instead of $\pi/2$,

$$\theta(z) = \theta_0 \left(1 - \frac{z}{L}\right) \quad \text{and} \quad \frac{d\theta}{dz} = -\frac{\theta_0}{L} \tag{5.22}$$

Using this, Equation (5.19) is replaced by

$$\phi(z) = \left[\frac{(e_1 - e_3)}{2} \frac{E\,L}{\theta_o\,K}\right] \Big[\theta(z)\cot\theta(z) - \theta_0(z)\cot\theta_0(z)\Big] \tag{5.23}$$

If θ_0 is very small, $\theta_0 \cot\theta_0 \simeq (1 - \theta_0^2/3)$, and

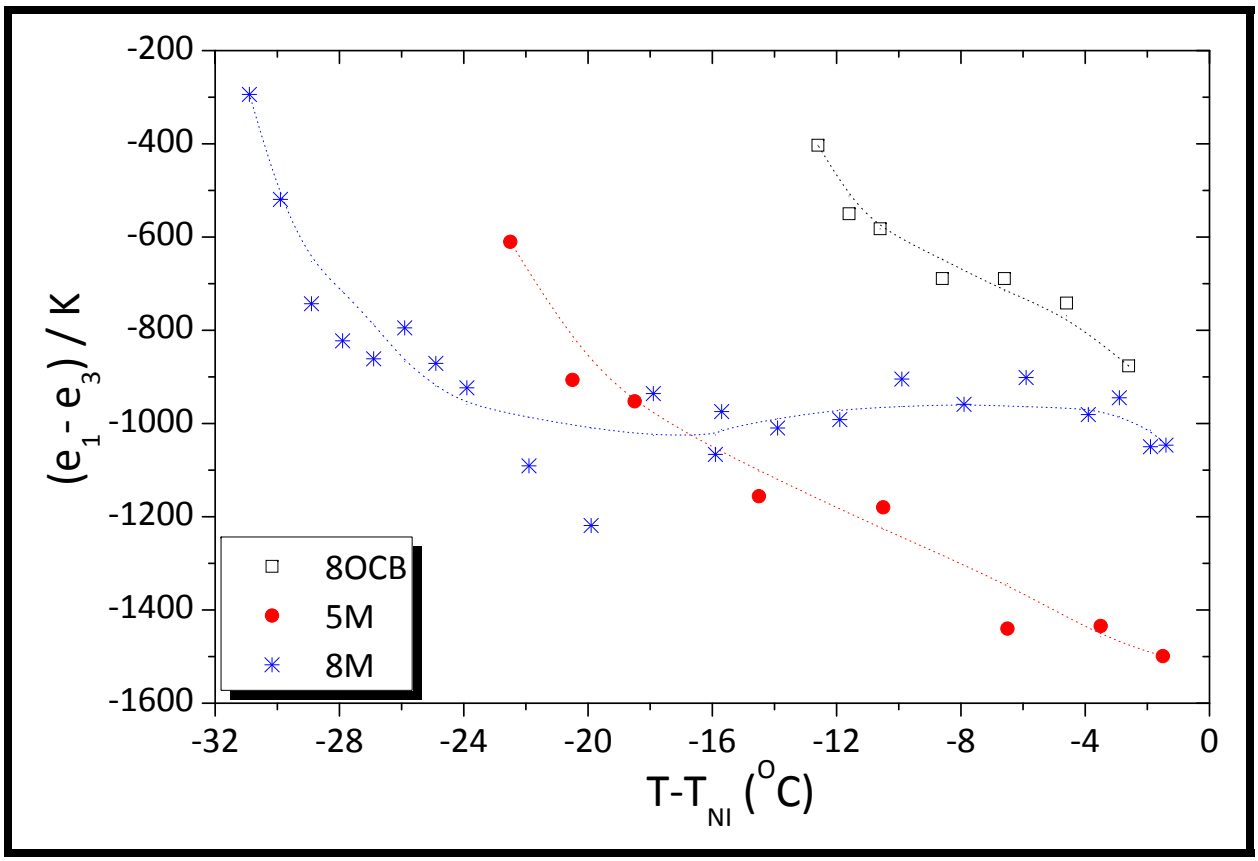

FIGURE 5.8: Variations of flexoelectric coefficient of pure 8OCB and two mixtures with relative temperature (using Equation (5.21), with $\theta_0 = \pi/2$; see text; the value for 8M is underestimated.)

$$\phi(L) \simeq \frac{(e_1 - e_3)\, E\, L}{6\, K}\, \theta_0 \tag{5.24}$$

or,

$$\left(\frac{e_1 - e_3}{K}\right) \simeq 6\, \frac{\phi(L)}{E\, L}\, \frac{1}{\theta_0} \tag{5.25}$$

ie., π of Equation (5.21) is replaced by $6/\theta_0$.

Assuming that $\theta_0 = \pi/2$ in 5M mixture, we estimate (e^*/K) due to BC molecules alone by the following relation :

$$\left(\frac{e^*}{K}\right)_{\text{Mix}} = \left(\frac{e^*}{K}\right)_{\text{8OCB}} C_{\text{8OCB}} + \left(\frac{e^*}{K}\right)_{\text{BC}} C_{\text{BC}} \tag{5.26}$$

where C_{8OCB} is the mol fraction of 8OCB and C_{BC} is the mol fraction of BC molecules. At $T - T_{NI} = -8^{\circ}$ C,

$$\left(\frac{e^*}{K}\right)_{Mix} = -1340, \left(\frac{e^*}{K}\right)_{8OCB} = -680 \quad \text{and} \quad C_{BC} = .05,\ C_{8OCB} = 0.95,$$

we get,

$$\boxed{\left(\frac{e^*}{K}\right)_{BC} \approx 20 \left(\frac{e^*}{K}\right)_{8OCB}} \tag{5.27}$$

$(e^*/K)_{BC}$ is much smaller than e_3/K value got by Harden *et al.* [75] in a different BC compound using a different technique.

Using Equation (5.26) and the value given in Equation (5.27), and the measurements on 8M mixture, we can estimate that $\theta_0 \simeq 1$ radian in this mixture. In the case of mixtures with higher compositions like 11M, θ_0 reduces fully to 0 and the sample is totally homeotropically aligned.

A possible reason for this trend is that in these cases $(e_1 - e_3)/K$ has extremely high values. As $(e_1 - e_3)$ increases, the polarization connected with the *splay-bend* distortion also increases. This polarization in turn creates an electric field **E** ($\simeq -4\pi$ **P**) whose vertical component in the center of the cell tends to realign the nematic director, acting on its dielectric anisotropy $\Delta\epsilon$. As $\Delta\epsilon > 0$, the vertical alignment is favoured, thus generating the homeotropic alignment seen in all samples with $>$ 11 Mol% of BC molecules in the hybrid aligned cell.

5.5 Conclusions

Our measurements of (e^*/K) in 8OCB and two mixtures 5M and 8M show that (i) the BC molecule has a much larger flexoelectric coefficient than that of a rod like molecule like 8OCB. The main contribution to e^* should be of dipolar origin, as originally envisaged by Meyer(see Figure 5.2). However the estimated value of e^* is much smaller than that on a pure compound. The large value in the latter case may be due to enhancement by cluster formation, which is essentially absent in our mixtures 5M and 8M. (ii) The relatively large value of (e^*/K) of the

BC molecules also gives rise to an increased internal field in the hybrid aligned cell when the concentration of BC molecules is increased. This in turn leads to a full reorientation of the director on the plate treated for planar alignment to give only homeotropically aligned cells for concentrations $>$ 11 Mol% of BC molecules.